Tunable synaptic devices based on ambipolar $MoTe_2$ transistor

Tingting Gao[1], Xuefei Li[1], Linxin Han[1] and Yanqing Wu[1,2*]

[1]Wuhan National High Magnetic Field Center and School of Optical and Electronic Information, Huazhong University of Science and Technology, Wuhan 430074, China,

[2]Institute of Microelectronics and Key Laboratory of Microelectronic Devices and Circuits (MOE), Peking University, Beijing 100871, China, *E-mail: yqwu@pku.edu.cn

Abstract

Synapse is one of the main elements of hardware implementation in a neuron network. Complex CMOS technology-based circuits using various Si-based transistors, non-Si based memory devices like RRAM, and 2D FET devices serve as hardware implement for neuron network. In this work, we demonstrate ambipolar $MoTe_2$ FET devices with a wide range of tunability in synaptic characteristic and classical paired pulsed facilitation as well as spike-timing-dependent plasticity function.

(Keywords: $MoTe_2$, synapse, spike-timing-dependent plasticity)

Introduction

Classical system has advantage in high speed and accuracy for specific problems, while biological systems are neat, fault tolerant, and energy efficient for complex bio-social events like visual and speech recognition, and locomotion control. In neural science, synapses functionally links neurons forming the path through which information flows. Synaptic weight means the connection strength of synapse between two neurons, presenting the firing probability on the post-neuron on the influence of pre-synapse [1]-[3]. To be specific, excitatory postsynaptic potential makes postsynaptic neuron more likely to fire while the inhibitory makes postsynaptic neuron less likely to fire and correspondingly the synapse weight means the likelihood [4]. Few layer $MoTe_2$ can be grown by chemical vapor deposition, which provides potential for wafer-scale integration and uniformity [6]. Furthermore, the native molybdenum oxide (MoO_x) typically forming together with $MoTe_2$ provides a natural oxide/semiconductor interface ideal for neuron devices [7]. In this work, we propose a $MoTe_2$ base Field-Effect Transistor (FET) to mimic synapse in neuromorphic computing. Our device has the ability to dynamically reconfigure between excitatory and inhibitory with large range tunable weight change.

Results and Discuss

The few-layer $MoTe_2$ were mechanically exfoliated from bulk crystal and then transferred on a p++ Si substrate coated with 18 nm of atomic layer deposited HfLaO. Prior to device fabrication, the $MoTe_2$ films were soaked in acetone and isopropanol to remove tape residues. Source/drain metal contacts were formed by e-beam lithography, 20/50 nm Pt/Au metal deposition and lift-off process. The device was then annealed in a furnace at 553 K for 2 hours under vacuum. The electrical characterization was carried out in a lakeshore cryogenic probe station under 10^{-5} Torr using an Agilent B1500A parameter analyzer.

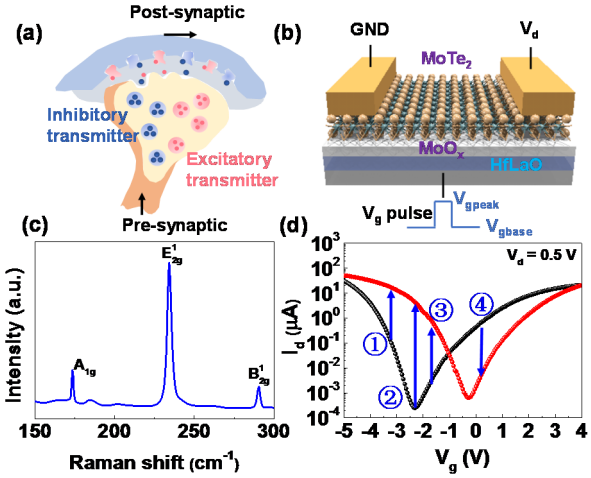

Fig. 1: (a) Biological schematic of synapse. (b) Schematic of the $MoTe_2$ back-gate FET. (c) Raman spectrum. (d) Transfer characteristic curve of $MoTe_2$ FET.

Figure 1(a) shows the schematic of biological synapse which can release excitatory or inhibitory neurotransmitters. The schematic of device structure and bias condition is presented in Figure 1(b). In the $MoTe_2$-based back gated FET, the presynaptic signal is applied at the back gate. The presynaptic signal contains two points of information. One is the base value (V_{gbase}) and the other is the peak value (V_{gpeak}) of the pulse, which can be considered to be a superposition of a constant voltage and a pure pulse voltage [8], [9]. The constant voltage controls the excitation or inhabitation state and the corresponding weight change in a wide range of the synaptic device while the pure pulse voltage determines the occurrence of the signal. The postsynaptic current (PSC) flows through the channel between source and drain, depending on the combined effect of V_{gbase} and V_{gpeak}. A thin native oxide of molybdenum exists between the $MoTe_2$ layer and the high-k gate

2021 5th IEEE Electron Devices Technology & Manufacturing Conference (EDTM) | 978-1-7281-8176-9/21/$31.00 ©2021 IEEE | DOI: 10.1109/EDTM50988.2021.9421022

dielectric. This MoO_x layer functions as the charge trapping or holding layer to achieve synaptic behavior in the device [10], [11]. The Raman spectrum of the transferred $MoTe_2$ for one of the devices is shown in Figure 1(c) [12]. Figure 1(d) shows the transfer characteristic curves of ambipolar $MoTe_2$ FET.

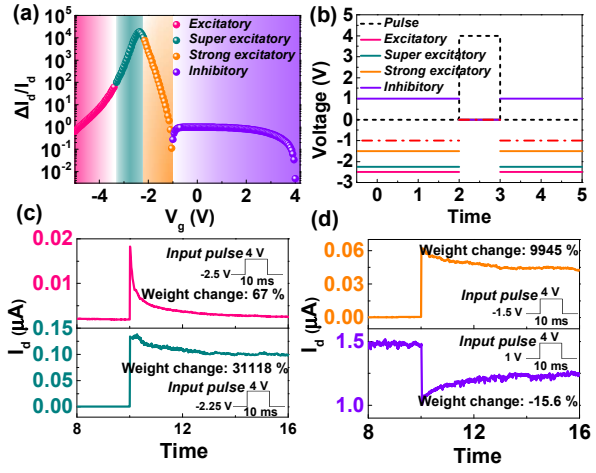

Fig. 2: (a) The current change ratio ($\Delta I_d / I_d$) as a function of V_g. (b) Bias condition of synaptic characterization. (c), (d) Single pulse responding of the synapse device.

Figure 2 shows the tunability of the device synaptic characteristics with control at V_{gbase} on the presynaptic terminal. As V_{gbase} sweeps bidirectionally between -4V to 4V, the current difference between forward bias and backward bias is displayed in Figure 2(a), where the influence caused by bias direction is equivalent to a pulse voltage shown in Figure 2(b). In Figure 2(c), (d), the current difference is plotted in logarithmic scale using its absolute value. Based on the distribution of current difference at diverse V_{gbase}, the plot is divided into four partitions, which is excitatory, super excitatory, strong excitatory and inhibitory partition respectively.

As a synapse device, conventional measurements like paired pulsed facilitation (PPF) and paired pulsed depression (PPD), single pulse-width modulation, spike-timing-dependent plasticity (STDP) are performed and shown in Figure 3,4. Paired pulsed measurement is performed in short-term synaptic mode. The device is generated by a pair of pulse with internal time from 30 ms to 1000 ms. For PPF, the amplitude of pulse voltage is of 4 V while for PPD is -4 V. Figure 3(a) shows a representative paired pulsed facilitation (PPF) of synaptic device, with internal time of 40 ms and PPF ratio of 446%. The maximum value of PPF ratio for this device is 562% when the internal time is of 30 ms. As the internal time increases, PPF ratio decline rapidly to 100% in 200 ms, and remain unchanged until 1000 ms (Figure 3(b)). Figure 3(c) shows a representative paired pulsed depression (PPD) of the synaptic device, with internal time of 100 ms and PPF ratio of 97%. The minimal value of PPD ratio for this device is 90% when the internal time is of 60 ms. As the internal time increases, PPD ratio rises rapidly to 100% in 200 ms, and remains unchanged until 1000 ms (Figure 3(d)).

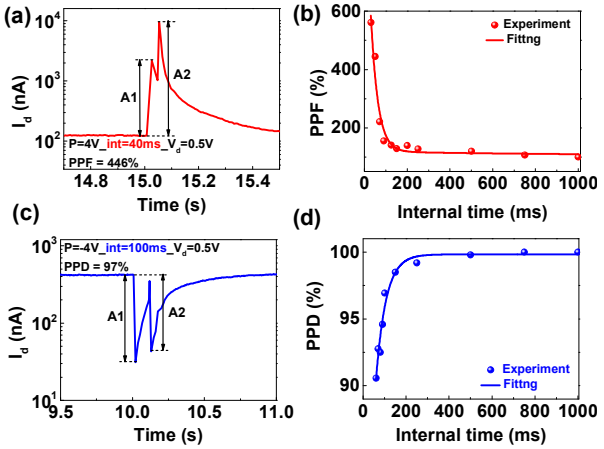

Fig. 3: (a) PPF performance of synaptic device. (b) PPF ratio as a function of internal time. (c) PPD performance of synaptic device. (d) PPF ratio as a function of internal time.

As shown in Figure 4(a), the arrival of presynaptic input pulse before the postsynaptic pulse weakens the synaptic connection (depression) with negative weight change and vice versa. The behavior of STDP can be described in exponential function $WC(\Delta t) = A_+ \exp(\Delta t / \tau_+)$,$\Delta t>0$; $A_- \exp(\Delta t / \tau_-)$, $\Delta t<0$ [10]. The width of input pulse means the degree of Fermi level shifting. Within the limits, the larger width of input pulse, the more the Fermi level shifts. In Figure 4(b), the weight change increases in an excitation mode. With the width of input pulse increase from 5 ms to 100 ms, the weight change of the device raising from 6.2% ~ 11%. In Figure 4(c), the weight change increases in an inhibition mode. With the width of input pulse increase from 5 ms to 100 ms, the weight change of the device drops from -7.4% ~ -30% and saturates at around -30% when the width reaches 50 ms.

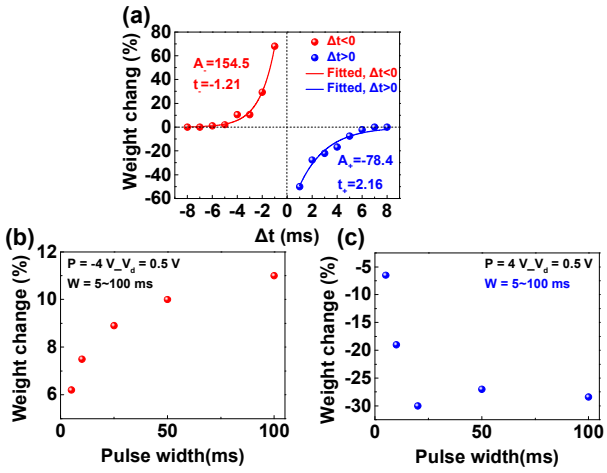

Fig. 4: (a) Spike-timing-dependent plasticity (STDP) characteristic in long-term plasticity. (b) Schematic of positive weight change as a function pulse width. (c) Schematic of negative weight change as a function pulse width.

Conclusion

In conclusion, we used $MoTe_2$-based electronic devices to emulate the function of synapse. Our work proposes a new perspective to mimic synapse using 3-terminal electronic devices. The characteristics of reconfigurable between the excitatory and inhibitory responses in a large span of weight change correspond well with biological activities. Conventional synaptic function of paired pulsed facilitation and spike-timing-dependent plasticity has also been demonstrated.

Acknowledgments

This work was supported by the Natural Science Foundation of China (Grant No. 91964106 and 61874162) and the 111 Project (B18001).

References

[1] S. Royer and D. Paré, "Conservation of total synaptic weight through balanced synaptic depression and potentiation," *Nature,* vol. 422, p. 518, 2003.

[2] V. M. Ho, J.-A. Lee, and K. C. Martin, "The Cell Biology of Synaptic Plasticity," *Science,* vol. 334, no. 6056, p. 623, 2011.

[3] L. F. Abbott, J. A. Varela, K. Sen, and S. B. Nelson, "Synaptic Depression and Cortical Gain Control," *Science,* vol. 275, no. 5297, p. 221, 1997.

[4] K. Duygu, Y. Shimeng, and H. S. P. Wong, "Synaptic electronics: materials, devices and applications," *Nanotechnology,* vol. 24, no. 38, p. 382001, 2013.

[5] Y.-F. Lin *et al.*, "Ambipolar $MoTe_2$ Transistors and Their Applications in Logic Circuits," vol. 26, no. 20, pp. 3263-3269, 2014.

[6] L. Zhou et al., "Large-Area Synthesis of High-Quality Uniform Few-Layer $MoTe_2$," Journal of the American Chemical Society, vol. 137, no. 37, pp. 11892-11895, 2015.

[7] G. Mirabelli *et al.*, "Air sensitivity of MoS_2, $MoSe_2$, $MoTe_2$, HfS_2, and $HfSe_2$," vol. 120, no. 12, p. 125102, 2016.

[8] C. S. Yang *et al.*, "A Synaptic Transistor based on Quasi-2D Molybdenum Oxide," *Advanced Materials,* vol. 29, no. 27, p. 1700906, 2017.

[9] S. Wang *et al.*, "A MoS_2/PTCDA Hybrid Heterojunction Synapse with Efficient Photoelectric Dual Modulation and Versatility," *Advanced Materials,* vol. 0, no. 0, p. 1806227, 2018.

[10] H. Tian *et al.*, "Anisotropic Black Phosphorus Synaptic Device for Neuromorphic Applications," *Advanced Materials,* vol. 28, no. 25, pp. 4991-4997, 2016.

[11] H. Tian *et al.*, "Emulating Bilingual Synaptic Response Using a Junction-Based Artificial Synaptic Device," *ACS Nano,* vol. 11, no. 7, pp. 7156-7163, 2017.

[12] C. Ruppert, O. B. Aslan, and T. F. Heinz, "Optical Properties and Band Gap of Single- and Few-Layer $MoTe_2$ Crystals," *Nano Letters,* vol. 14, no. 11, pp. 6231-6236, 2014.